hep-ex/0408028
BABAR-CONF-04/013
SLAC-PUB-10615

Search for $b \to u$ Transitions in $B^- \to \overline{D}^0 K^-$ and $B^- \to \overline{D}^{*0} K^-$

The *BABAR* Collaboration

August 10, 2004

Abstract

We report on searches for $B^- \to \overline{D}^0 K^-$ and $B^- \to \overline{D}^{*0} K^-$, with $\overline{D}^{*0} \to \overline{D}^0 \pi^0$ or $\overline{D}^{*0} \to \overline{D}^0 \gamma$, and $\overline{D}^0 \to K^+\pi^-$ (and charge conjugates). These final states, which we denote as $[K^+\pi^-]_D K^-$ and $[K^+\pi^-]_{D^*} K^-$, can be reached through the $b \to c$ transition $B^- \to D^{(*)0} K^-$ followed by the doubly Cabibbo-suppressed $D^0 \to K^+\pi^-$, or through the $b \to u$ transition $B^- \to \overline{D}^{(*)0} K^-$ followed by the Cabibbo-favored $\overline{D}^0 \to K^+\pi^-$, or through interference of the two. Our results are based on 227 million $\Upsilon(4S) \to B\overline{B}$ decays collected with the *BABAR* detector at SLAC. We set preliminary limits on the ratios

$$\mathcal{R}_{K\pi} \equiv \frac{\Gamma(B^+ \to [K^-\pi^+]_D K^+) + \Gamma(B^- \to [K^+\pi^-]_D K^-)}{\Gamma(B^+ \to [K^+\pi^-]_D K^+) + \Gamma(B^- \to [K^-\pi^+]_D K^-)} < 0.030 \quad (90\%\ \text{C.L.})$$

and

$$\mathcal{R}^*{}_{K\pi} \equiv \frac{\Gamma(B^+ \to [K^-\pi^+]_{D^*} K^+) + \Gamma(B^- \to [K^+\pi^-]_{D^*} K^-)}{\Gamma(B^+ \to [K^+\pi^-]_{D^*} K^+) + \Gamma(B^- \to [K^-\pi^+]_{D^*} K^-)} < 0.021 \quad (90\%\ \text{C.L.}),$$

where the central values are $\mathcal{R}_{K\pi} = 0.013 \pm^{0.011}_{0.009}$ and $\mathcal{R}^*{}_{K\pi} = 0.003 \pm^{0.010}_{0.007}$. These limits constrain the amplitude ratios $r_B \equiv |A(B^- \to \overline{D}^0 K^-)/A(B^- \to D^0 K^-)| < 0.23$ and $r_B^* \equiv |A(B^- \to \overline{D}^{*0} K^-)/A(B^- \to D^{*0} K^-)| < 0.21$ at the 90% confidence level.

Submitted to the 32nd International Conference on High-Energy Physics, ICHEP 04,
16 August—22 August 2004, Beijing, China

Stanford Linear Accelerator Center, Stanford University, Stanford, CA 94309

Work supported in part by Department of Energy contract DE-AC03-76SF00515.

The *BABAR* Collaboration,

B. Aubert, R. Barate, D. Boutigny, F. Couderc, J.-M. Gaillard, A. Hicheur, Y. Karyotakis, J. P. Lees, V. Tisserand, A. Zghiche

Laboratoire de Physique des Particules, F-74941 Annecy-le-Vieux, France

A. Palano, A. Pompili

Università di Bari, Dipartimento di Fisica and INFN, I-70126 Bari, Italy

J. C. Chen, N. D. Qi, G. Rong, P. Wang, Y. S. Zhu

Institute of High Energy Physics, Beijing 100039, China

G. Eigen, I. Ofte, B. Stugu

University of Bergen, Inst. of Physics, N-5007 Bergen, Norway

G. S. Abrams, A. W. Borgland, A. B. Breon, D. N. Brown, J. Button-Shafer, R. N. Cahn, E. Charles, C. T. Day, M. S. Gill, A. V. Gritsan, Y. Groysman, R. G. Jacobsen, R. W. Kadel, J. Kadyk, L. T. Kerth, Yu. G. Kolomensky, G. Kukartsev, G. Lynch, L. M. Mir, P. J. Oddone, T. J. Orimoto, M. Pripstein, N. A. Roe, M. T. Ronan, V. G. Shelkov, W. A. Wenzel

Lawrence Berkeley National Laboratory and University of California, Berkeley, CA 94720, USA

M. Barrett, K. E. Ford, T. J. Harrison, A. J. Hart, C. M. Hawkes, S. E. Morgan, A. T. Watson

University of Birmingham, Birmingham, B15 2TT, United Kingdom

M. Fritsch, K. Goetzen, T. Held, H. Koch, B. Lewandowski, M. Pelizaeus, M. Steinke

Ruhr Universität Bochum, Institut für Experimentalphysik 1, D-44780 Bochum, Germany

J. T. Boyd, N. Chevalier, W. N. Cottingham, M. P. Kelly, T. E. Latham, F. F. Wilson

University of Bristol, Bristol BS8 1TL, United Kingdom

T. Cuhadar-Donszelmann, C. Hearty, N. S. Knecht, T. S. Mattison, J. A. McKenna, D. Thiessen

University of British Columbia, Vancouver, BC, Canada V6T 1Z1

A. Khan, P. Kyberd, L. Teodorescu

Brunel University, Uxbridge, Middlesex UB8 3PH, United Kingdom

A. E. Blinov, V. E. Blinov, V. P. Druzhinin, V. B. Golubev, V. N. Ivanchenko, E. A. Kravchenko, A. P. Onuchin, S. I. Serednyakov, Yu. I. Skovpen, E. P. Solodov, A. N. Yushkov

Budker Institute of Nuclear Physics, Novosibirsk 630090, Russia

D. Best, M. Bruinsma, M. Chao, I. Eschrich, D. Kirkby, A. J. Lankford, M. Mandelkern, R. K. Mommsen, W. Roethel, D. P. Stoker

University of California at Irvine, Irvine, CA 92697, USA

C. Buchanan, B. L. Hartfiel

University of California at Los Angeles, Los Angeles, CA 90024, USA

S. D. Foulkes, J. W. Gary, B. C. Shen, K. Wang

University of California at Riverside, Riverside, CA 92521, USA

D. del Re, H. K. Hadavand, E. J. Hill, D. B. MacFarlane, H. P. Paar, Sh. Rahatlou, V. Sharma

University of California at San Diego, La Jolla, CA 92093, USA

J. W. Berryhill, C. Campagnari, B. Dahmes, O. Long, A. Lu, M. A. Mazur, J. D. Richman, W. Verkerke

University of California at Santa Barbara, Santa Barbara, CA 93106, USA

T. W. Beck, A. M. Eisner, C. A. Heusch, J. Kroseberg, W. S. Lockman, G. Nesom, T. Schalk, B. A. Schumm, A. Seiden, P. Spradlin, D. C. Williams, M. G. Wilson

University of California at Santa Cruz, Institute for Particle Physics, Santa Cruz, CA 95064, USA

J. Albert, E. Chen, G. P. Dubois-Felsmann, A. Dvoretskii, D. G. Hitlin, I. Narsky, T. Piatenko, F. C. Porter, A. Ryd, A. Samuel, S. Yang

California Institute of Technology, Pasadena, CA 91125, USA

S. Jayatilleke, G. Mancinelli, B. T. Meadows, M. D. Sokoloff

University of Cincinnati, Cincinnati, OH 45221, USA

T. Abe, F. Blanc, P. Bloom, S. Chen, W. T. Ford, U. Nauenberg, A. Olivas, P. Rankin, J. G. Smith, J. Zhang, L. Zhang

University of Colorado, Boulder, CO 80309, USA

A. Chen, J. L. Harton, A. Soffer, W. H. Toki, R. J. Wilson, Q. Zeng

Colorado State University, Fort Collins, CO 80523, USA

D. Altenburg, T. Brandt, J. Brose, M. Dickopp, E. Feltresi, A. Hauke, H. M. Lacker, R. Müller-Pfefferkorn, R. Nogowski, S. Otto, A. Petzold, J. Schubert, K. R. Schubert, R. Schwierz, B. Spaan, J. E. Sundermann

Technische Universität Dresden, Institut für Kern- und Teilchenphysik, D-01062 Dresden, Germany

D. Bernard, G. R. Bonneaud, F. Brochard, P. Grenier, S. Schrenk, Ch. Thiebaux, G. Vasileiadis, M. Verderi

Ecole Polytechnique, LLR, F-91128 Palaiseau, France

D. J. Bard, P. J. Clark, D. Lavin, F. Muheim, S. Playfer, Y. Xie

University of Edinburgh, Edinburgh EH9 3JZ, United Kingdom

M. Andreotti, V. Azzolini, D. Bettoni, C. Bozzi, R. Calabrese, G. Cibinetto, E. Luppi, M. Negrini, L. Piemontese, A. Sarti

Università di Ferrara, Dipartimento di Fisica and INFN, I-44100 Ferrara, Italy

E. Treadwell

Florida A&M University, Tallahassee, FL 32307, USA

F. Anulli, R. Baldini-Ferroli, A. Calcaterra, R. de Sangro, G. Finocchiaro, P. Patteri, I. M. Peruzzi, M. Piccolo, A. Zallo

Laboratori Nazionali di Frascati dell'INFN, I-00044 Frascati, Italy

A. Buzzo, R. Capra, R. Contri, G. Crosetti, M. Lo Vetere, M. Macri, M. R. Monge, S. Passaggio, C. Patrignani, E. Robutti, A. Santroni, S. Tosi

Università di Genova, Dipartimento di Fisica and INFN, I-16146 Genova, Italy

S. Bailey, G. Brandenburg, K. S. Chaisanguanthum, M. Morii, E. Won

Harvard University, Cambridge, MA 02138, USA

R. S. Dubitzky, U. Langenegger

Universität Heidelberg, Physikalisches Institut, Philosophenweg 12, D-69120 Heidelberg, Germany

W. Bhimji, D. A. Bowerman, P. D. Dauncey, U. Egede, J. R. Gaillard, G. W. Morton, J. A. Nash, M. B. Nikolich, G. P. Taylor

Imperial College London, London, SW7 2AZ, United Kingdom

M. J. Charles, G. J. Grenier, U. Mallik

University of Iowa, Iowa City, IA 52242, USA

J. Cochran, H. B. Crawley, J. Lamsa, W. T. Meyer, S. Prell, E. I. Rosenberg, A. E. Rubin, J. Yi

Iowa State University, Ames, IA 50011-3160, USA

M. Biasini, R. Covarelli, M. Pioppi

Università di Perugia, Dipartimento di Fisica and INFN, I-06100 Perugia, Italy

M. Davier, X. Giroux, G. Grosdidier, A. Höcker, S. Laplace, F. Le Diberder, V. Lepeltier, A. M. Lutz, T. C. Petersen, S. Plaszczynski, M. H. Schune, L. Tantot, G. Wormser

Laboratoire de l'Accélérateur Linéaire, F-91898 Orsay, France

C. H. Cheng, D. J. Lange, M. C. Simani, D. M. Wright

Lawrence Livermore National Laboratory, Livermore, CA 94550, USA

A. J. Bevan, C. A. Chavez, J. P. Coleman, I. J. Forster, J. R. Fry, E. Gabathuler, R. Gamet, D. E. Hutchcroft, R. J. Parry, D. J. Payne, R. J. Sloane, C. Touramanis

University of Liverpool, Liverpool L69 72E, United Kingdom

J. J. Back,[1] C. M. Cormack, P. F. Harrison,[1] F. Di Lodovico, G. B. Mohanty[1]

Queen Mary, University of London, E1 4NS, United Kingdom

C. L. Brown, G. Cowan, R. L. Flack, H. U. Flaecher, M. G. Green, P. S. Jackson, T. R. McMahon, S. Ricciardi, F. Salvatore, M. A. Winter

University of London, Royal Holloway and Bedford New College, Egham, Surrey TW20 0EX, United Kingdom

D. Brown, C. L. Davis

University of Louisville, Louisville, KY 40292, USA

J. Allison, N. R. Barlow, R. J. Barlow, P. A. Hart, M. C. Hodgkinson, G. D. Lafferty, A. J. Lyon, J. C. Williams

University of Manchester, Manchester M13 9PL, United Kingdom

A. Farbin, W. D. Hulsbergen, A. Jawahery, D. Kovalskyi, C. K. Lae, V. Lillard, D. A. Roberts

University of Maryland, College Park, MD 20742, USA

G. Blaylock, C. Dallapiccola, K. T. Flood, S. S. Hertzbach, R. Kofler, V. B. Koptchev, T. B. Moore, S. Saremi, H. Staengle, S. Willocq

University of Massachusetts, Amherst, MA 01003, USA

[1]Now at Department of Physics, University of Warwick, Coventry, United Kingdom

R. Cowan, G. Sciolla, S. J. Sekula, F. Taylor, R. K. Yamamoto

Massachusetts Institute of Technology, Laboratory for Nuclear Science, Cambridge, MA 02139, USA

D. J. J. Mangeol, P. M. Patel, S. H. Robertson

McGill University, Montréal, QC, Canada H3A 2T8

A. Lazzaro, V. Lombardo, F. Palombo

Università di Milano, Dipartimento di Fisica and INFN, I-20133 Milano, Italy

J. M. Bauer, L. Cremaldi, V. Eschenburg, R. Godang, R. Kroeger, J. Reidy, D. A. Sanders, D. J. Summers, H. W. Zhao

University of Mississippi, University, MS 38677, USA

S. Brunet, D. Côté, P. Taras

Université de Montréal, Laboratoire René J. A. Lévesque, Montréal, QC, Canada H3C 3J7

H. Nicholson

Mount Holyoke College, South Hadley, MA 01075, USA

N. Cavallo,[2] F. Fabozzi,[2] C. Gatto, L. Lista, D. Monorchio, P. Paolucci, D. Piccolo, C. Sciacca

Università di Napoli Federico II, Dipartimento di Scienze Fisiche and INFN, I-80126, Napoli, Italy

M. Baak, H. Bulten, G. Raven, H. L. Snoek, L. Wilden

NIKHEF, National Institute for Nuclear Physics and High Energy Physics, NL-1009 DB Amsterdam, The Netherlands

C. P. Jessop, J. M. LoSecco

University of Notre Dame, Notre Dame, IN 46556, USA

T. Allmendinger, K. K. Gan, K. Honscheid, D. Hufnagel, H. Kagan, R. Kass, T. Pulliam, A. M. Rahimi, R. Ter-Antonyan, Q. K. Wong

Ohio State University, Columbus, OH 43210, USA

J. Brau, R. Frey, O. Igonkina, C. T. Potter, N. B. Sinev, D. Strom, E. Torrence

University of Oregon, Eugene, OR 97403, USA

F. Colecchia, A. Dorigo, F. Galeazzi, M. Margoni, M. Morandin, M. Posocco, M. Rotondo, F. Simonetto, R. Stroili, G. Tiozzo, C. Voci

Università di Padova, Dipartimento di Fisica and INFN, I-35131 Padova, Italy

M. Benayoun, H. Briand, J. Chauveau, P. David, Ch. de la Vaissière, L. Del Buono, O. Hamon, M. J. J. John, Ph. Leruste, J. Malcles, J. Ocariz, M. Pivk, L. Roos, S. T'Jampens, G. Therin

Universités Paris VI et VII, Laboratoire de Physique Nucléaire et de Hautes Energies, F-75252 Paris, France

P. F. Manfredi, V. Re

Università di Pavia, Dipartimento di Elettronica and INFN, I-27100 Pavia, Italy

[2]Also with Università della Basilicata, Potenza, Italy

P. K. Behera, L. Gladney, Q. H. Guo, J. Panetta

University of Pennsylvania, Philadelphia, PA 19104, USA

C. Angelini, G. Batignani, S. Bettarini, M. Bondioli, F. Bucci, G. Calderini, M. Carpinelli, F. Forti, M. A. Giorgi, A. Lusiani, G. Marchiori, F. Martinez-Vidal,[3] M. Morganti, N. Neri, E. Paoloni, M. Rama, G. Rizzo, F. Sandrelli, J. Walsh

Università di Pisa, Dipartimento di Fisica, Scuola Normale Superiore and INFN, I-56127 Pisa, Italy

M. Haire, D. Judd, K. Paick, D. E. Wagoner

Prairie View A&M University, Prairie View, TX 77446, USA

N. Danielson, P. Elmer, Y. P. Lau, C. Lu, V. Miftakov, J. Olsen, A. J. S. Smith, A. V. Telnov

Princeton University, Princeton, NJ 08544, USA

F. Bellini, G. Cavoto,[4] R. Faccini, F. Ferrarotto, F. Ferroni, M. Gaspero, L. Li Gioi, M. A. Mazzoni, S. Morganti, M. Pierini, G. Piredda, F. Safai Tehrani, C. Voena

Università di Roma La Sapienza, Dipartimento di Fisica and INFN, I-00185 Roma, Italy

S. Christ, G. Wagner, R. Waldi

Universität Rostock, D-18051 Rostock, Germany

T. Adye, N. De Groot, B. Franek, N. I. Geddes, G. P. Gopal, E. O. Olaiya

Rutherford Appleton Laboratory, Chilton, Didcot, Oxon, OX11 0QX, United Kingdom

R. Aleksan, S. Emery, A. Gaidot, S. F. Ganzhur, P.-F. Giraud, G. Hamel de Monchenault, W. Kozanecki, M. Legendre, G. W. London, B. Mayer, G. Schott, G. Vasseur, Ch. Yèche, M. Zito

DSM/Dapnia, CEA/Saclay, F-91191 Gif-sur-Yvette, France

M. V. Purohit, A. W. Weidemann, J. R. Wilson, F. X. Yumiceva

University of South Carolina, Columbia, SC 29208, USA

D. Aston, R. Bartoldus, N. Berger, A. M. Boyarski, O. L. Buchmueller, R. Claus, M. R. Convery, M. Cristinziani, G. De Nardo, D. Dong, J. Dorfan, D. Dujmic, W. Dunwoodie, E. E. Elsen, S. Fan, R. C. Field, T. Glanzman, S. J. Gowdy, T. Hadig, V. Halyo, C. Hast, T. Hryn'ova, W. R. Innes, M. H. Kelsey, P. Kim, M. L. Kocian, D. W. G. S. Leith, J. Libby, S. Luitz, V. Luth, H. L. Lynch, H. Marsiske, R. Messner, D. R. Muller, C. P. O'Grady, V. E. Ozcan, A. Perazzo, M. Perl, S. Petrak, B. N. Ratcliff, A. Roodman, A. A. Salnikov, R. H. Schindler, J. Schwiening, G. Simi, A. Snyder, A. Soha, J. Stelzer, D. Su, M. K. Sullivan, J. Va'vra, S. R. Wagner, M. Weaver, A. J. R. Weinstein, W. J. Wisniewski, M. Wittgen, D. H. Wright, A. K. Yarritu, C. C. Young

Stanford Linear Accelerator Center, Stanford, CA 94309, USA

P. R. Burchat, A. J. Edwards, T. I. Meyer, B. A. Petersen, C. Roat

Stanford University, Stanford, CA 94305-4060, USA

S. Ahmed, M. S. Alam, J. A. Ernst, M. A. Saeed, M. Saleem, F. R. Wappler

State University of New York, Albany, NY 12222, USA

[3]Also with IFIC, Instituto de Física Corpuscular, CSIC-Universidad de Valencia, Valencia, Spain
[4]Also with Princeton University, Princeton, USA

W. Bugg, M. Krishnamurthy, S. M. Spanier
University of Tennessee, Knoxville, TN 37996, USA

R. Eckmann, H. Kim, J. L. Ritchie, A. Satpathy, R. F. Schwitters
University of Texas at Austin, Austin, TX 78712, USA

J. M. Izen, I. Kitayama, X. C. Lou, S. Ye
University of Texas at Dallas, Richardson, TX 75083, USA

F. Bianchi, M. Bona, F. Gallo, D. Gamba
Università di Torino, Dipartimento di Fisica Sperimentale and INFN, I-10125 Torino, Italy

L. Bosisio, C. Cartaro, F. Cossutti, G. Della Ricca, S. Dittongo, S. Grancagnolo, L. Lanceri, P. Poropat,[5] L. Vitale, G. Vuagnin
Università di Trieste, Dipartimento di Fisica and INFN, I-34127 Trieste, Italy

R. S. Panvini
Vanderbilt University, Nashville, TN 37235, USA

Sw. Banerjee, C. M. Brown, D. Fortin, P. D. Jackson, R. Kowalewski, J. M. Roney, R. J. Sobie
University of Victoria, Victoria, BC, Canada V8W 3P6

H. R. Band, B. Cheng, S. Dasu, M. Datta, A. M. Eichenbaum, M. Graham, J. J. Hollar, J. R. Johnson, P. E. Kutter, H. Li, R. Liu, A. Mihalyi, A. K. Mohapatra, Y. Pan, R. Prepost, P. Tan, J. H. von Wimmersperg-Toeller, J. Wu, S. L. Wu, Z. Yu
University of Wisconsin, Madison, WI 53706, USA

M. G. Greene, H. Neal
Yale University, New Haven, CT 06511, USA

[5]Deceased

1 INTRODUCTION

Following the discovery of *CP* violation in B-meson decays and the measurement of the angle β of the unitarity triangle [1] associated with the Cabibbo-Kobayashi-Maskawa (CKM) quark mixing matrix, focus has turned towards the measurements of the other angles α and γ. The angle γ is $\arg(-V_{ub}^* V_{ud}/V_{cb}^* V_{cd})$, where V_{ij} are CKM matrix elements; in the Wolfenstein convention [2], $\gamma = \arg(V_{ub}^*)$.

Several proposed methods for measuring γ exploit the interference between $B^- \to D^{(*)0} K^{(*)-}$ and $B^- \to \overline{D}^{(*)0} K^{(*)-}$ (Fig. 1) which occurs when the $D^{(*)0}$ and the $\overline{D}^{(*)0}$ decay to common final states, as first suggested in Ref. [3].

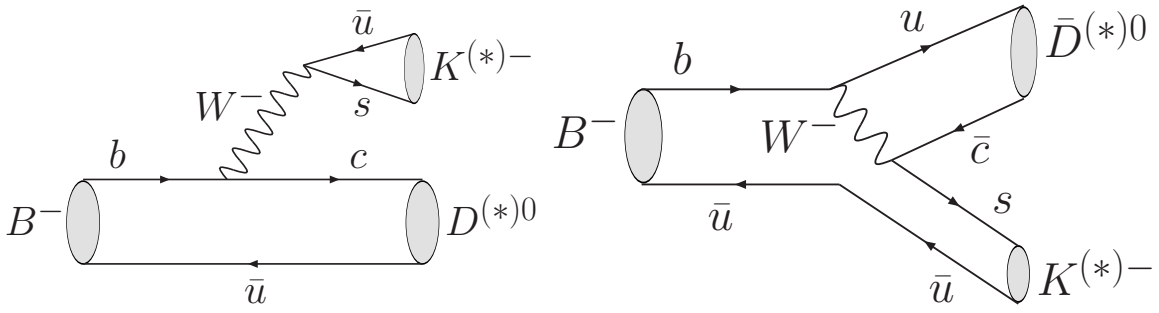

Figure 1: Feynman diagrams for $B^- \to D^{(*)0} K^{(*)-}$ and $\overline{D}^{(*)0} K^{(*)-}$. The latter is CKM- and color-suppressed with respect to the former. The CKM and color suppression factors are expected to be roughly $|V_{ub} V_{cs}^* / V_{cb} V_{us}^*| \approx 0.4$ and 1/3 respectively.

As proposed in Ref. [4], we search for $B^- \to \overline{D}^0 K^-$ and $B^- \to \overline{D}^{*0} K^-$, $\overline{D}^{*0} \to \overline{D}^0 \pi^0/\gamma$ followed by $\overline{D}^0 \to K^+\pi^-$, as well as the charge conjugate sequences. In these processes, the favored B decay followed by the doubly CKM-suppressed D decay interferes with the suppressed B decay followed by the CKM-favored D decay. The interference of the $b \to c$ and $b \to u$ amplitudes is sensitive to the relative weak phase $\gamma \equiv \arg(-V_{ud} V_{ub}^* / V_{cd} V_{cb}^*)$.

We use the notation $B^- \to [h_1^+ h_2^-]_D h_3^-$ (with each $h_i = \pi$ or K) for the decay chain $B^- \to \overline{D}^0 h_3^-$, $\overline{D}^0 \to h_1^+ h_2^-$. For the closely related modes with a $\overline{D}^{*0}$, we use the same notation with the subscript D replaced by D^*. We also refer to h_3 as the bachelor π or K.

In the decays of interest, the sign of the bachelor kaon is opposite to that of the kaon from D decay. It is convenient to define ratios of rates between these decays and the similar decays where the two kaons have the same sign. The decays with same-sign kaons have much higher rate and proceed almost exclusively through the CKM-favored and color favored B transition, followed by the Cabibbo-favored D-decay. The advantage in taking ratios is that most theoretical and experimental uncertainties cancel. Thus, ignoring the possible effects of D mixing, we define the charge-specific ratios for D and D^* as:

$$\mathcal{R}_{K\pi}^{\pm} \equiv \frac{\Gamma([K^{\mp}\pi^{\pm}]_D K^{\pm})}{\Gamma([K^{\pm}\pi^{\mp}]_D K^{\pm})} = r_B^2 + r_D^2 + 2 r_B r_D \cos(\pm\gamma + \delta) \tag{1}$$

and

$$\mathcal{R}_{K\pi}^{*\pm} \equiv \frac{\Gamma([K^{\mp}\pi^{\pm}]_{D^*} K^{\pm})}{\Gamma([K^{\pm}\pi^{\mp}]_{D^*} K^{\pm})} = r_B^{*2} + r_D^2 + 2 r_B^* r_D \cos(\pm\gamma + \delta^*), \tag{2}$$

where

$$r_B \equiv \left| \frac{A(B^- \to \overline{D}^0 K^-)}{A(B^- \to D^0 K^-)} \right|, \tag{3}$$

$$r_B^* \equiv \left| \frac{A(B^- \to \overline{D}^{*0} K^-)}{A(B^- \to D^{*0} K^-)} \right|, \tag{4}$$

$$r_D \equiv \left| \frac{A(D^0 \to K^+\pi^-)}{A(D^0 \to K^-\pi^+)} \right| = 0.060 \pm 0.003 \text{ [5]}, \tag{5}$$

$$\delta^{(*)} \equiv \delta_B^{(*)} + \delta_D, \tag{6}$$

and $\delta_B^{(*)}$ and δ_D are strong phase differences between the two B and D decay amplitudes, respectively.

We also define the charge-integrated ratios:

$$\mathcal{R}_{K\pi} \equiv \frac{\Gamma(B^- \to [K^+\pi^-]_D K^-) + \Gamma(B^+ \to [K^-\pi^+]_D K^+)}{\Gamma(B^- \to [K^-\pi^+]_D K^-) + \Gamma(B^+ \to [K^+\pi^-]_D K^+)} \tag{7}$$

and

$$\mathcal{R}_{K\pi}^* \equiv \frac{\Gamma(B^- \to [K^+\pi^-]_{D^*} K^-) + \Gamma(B^+ \to [K^-\pi^+]_{D^*} K^+)}{\Gamma(B^- \to [K^-\pi^+]_{D^*} K^-) + \Gamma(B^+ \to [K^+\pi^-]_{D^*} K^+)}. \tag{8}$$

Then,

$$\mathcal{R}_{K\pi}^{(*)} = \frac{\mathcal{R}_{K\pi}^{(*)+} + \mathcal{R}_{K\pi}^{(*)-}}{2} = r_B^{(*)2} + r_D^2 + 2 r_B^{(*)} r_D \cos\gamma \cos\delta^{(*)}, \tag{9}$$

assuming no CP violation in the normalization modes $[K^\mp\pi^\pm]_D K^\mp$ and $[K^\mp\pi^\pm]_{D^*} K^\mp$.

Since $r_B^{(*)}$ is expected to be of the same order as r_D, CP violation could manifest itself as a large difference between the charge-specific ratios $\mathcal{R}_{K\pi}^{(*)+}$ and $\mathcal{R}_{K\pi}^{(*)-}$. Measurements of these four ratios are not sufficient to extract γ, since these quantities are expressed in terms of five unknowns: γ, r_B, δ, r_B^*, and δ^*. However, these measurements can be combined with information from other modes to extract γ, up to discrete ambiguities, in a theoretically clean way [4].

The value of $r_B^{(*)}$ determines, in part, the level of interference between the diagrams of Fig. 1. In most techniques for measuring γ, high values of $r_B^{(*)}$ lead to larger interference and better sensitivity to γ. As we will describe below, the measured $\mathcal{R}_{K\pi}^{(*)}$ are consistent with zero in the current analysis. This allows us to set restrictive upper limits on $r_B^{(*)}$, since $\mathcal{R}_{K\pi}^{(*)}$ depend quadratically on $r_B^{(*)}$.

In the Standard Model, $r_B^{(*)} = |V_{ub}V_{cs}^*/V_{cb}V_{us}^*| F_{cs} \approx 0.4 F_{cs}$. The color-suppression factor $F_{cs} < 1$ accounts for the additional suppression, beyond that due to CKM factors, of $B^- \to \overline{D}^{(*)0} K^-$ relative to $B^- \to D^{(*)0} K^-$. Naively, $F_{cs} = \frac{1}{3}$, which is the probability for the color of the quarks from the virtual W in $B^- \to \overline{D}^{(*)0} K^-$ to match that of the other two quarks; see Fig. 1. Early estimates [6] of F_{cs} were based on factorization and the then available experimental information on a number of $b \to c$ transitions. These estimates gave $F_{cs} \approx 0.22$, leading to $r_B^{(*)} \approx 0.09$. However, the recent observations and measurements [7] of color suppressed $b \to c$ decays ($B \to D^{(*)} h^0$; $h^0 = \pi^0, \rho^0, \omega, \eta, \eta'$) suggest that F_{cs}, and therefore $r_B^{(*)}$, could be larger.

In this paper we report on an update of our previous analysis of $B^- \to \overset{(-)}{D}{}^0 K^-$ [8], and the first attempt to study $B^- \to \overset{(-)}{D}{}^{*0} K^-$. The previous analysis was based on a sample of B-meson decays a factor of 1.9 smaller than used here, and resulted in an upper limit $\mathcal{R}_{K\pi} < 0.026$ at the 90%

confidence level. This in turn was translated into a limit $r_B < 0.22$, also at 90% C.L.. On the other hand, a study by the Belle collaboration [9] of $B^\pm \to \overset{(-)}{D}{}^0 K^\pm$ and $B^\pm \to \overset{(-)}{D}{}^{*0} K^\pm$, $\overset{(-)}{D}{}^0 \to K_S\pi^+\pi^-$, favors rather large color suppressed amplitudes: $r_B = 0.26^{+0.11}_{-0.15}$ and $r_B^* = 0.20^{+0.20}_{-0.18}$.

2 THE *BABAR* DATASET

The results presented in this paper are based on 227×10^6 $\Upsilon(4S) \to B\overline{B}$ decays, corresponding to an integrated luminosity of 205 fb^{-1}. The data were collected between 1999 and 2004 with the *BABAR* detector [10] at the PEP-II B Factory at SLAC [11]. In addition, a 16 fb^{-1} off-resonance data sample, with center-of-mass (CM) energy 40 MeV below the $\Upsilon(4S)$ resonance, is used to study backgrounds from continuum events, $e^+e^- \to q\bar{q}$ ($q = u, d, s$, or c).

3 ANALYSIS METHOD

This work is an extension of our analysis from Ref. [8], which resulted in limits on $\mathcal{R}_{K\pi} < 0.026$ and $r_B < 0.22$, as mentioned above. The main changes in the analysis are the following:

- The size of the dataset is increased from 120 to 227×10^6 $\Upsilon(4S) \to B\overline{B}$ decays.
- This analysis also includes the $B^\pm \to \overset{(-)}{D}{}^{*0} K^\pm$ mode.
- The analysis requirements have been tightened in order to reduce backgrounds further.
- A few of the requirements in the previous analysis resulted in small differences in the efficiencies of the signal mode $B^\pm \to [K^\mp\pi^\pm]K^\pm$ and the normalization mode $B^\pm \to [K^\pm\pi^\mp]K^\pm$. These requirements have now been removed.

Table 1: Notation used in the text.

Abbreviation	Mode	Comments
DK	$B^- \to D^0K^-$, $D^0 \to K^-\pi^+$ and c.c.	normalization mode
$D\pi$	$B^- \to D^0\pi^-$, $D^0 \to K^-\pi^+$ and c.c.	control mode
$\overline{D}K$	$B^- \to \overset{(-)}{D}{}^0K^-$, $\overset{(-)}{D}{}^0 \to K^+\pi^-$ and c.c.	signal mode
D^*K	$B^- \to D^{*0}K^-$, $D^{*0} \to D^0\pi^0/\gamma$, $D^0 \to K^-\pi^+$ and c.c.	normalization mode
$D^*\pi$	$B^- \to D^{*0}\pi^-$, $D^{*0} \to D^0\pi^0/\gamma$, $D^0 \to K^-\pi^+$ and c.c.	control mode
$\overline{D}^*K$	$B^- \to \overset{(-)}{D}{}^{*0}K^-$, $\overset{(-)}{D}{}^{*0} \to \overset{(-)}{D}{}^0\pi^0/\gamma$, $\overset{(-)}{D}{}^0 \to K^+\pi^-$ and c.c.	signal mode

The analysis makes use of several samples from different decay modes. Throughout the following discussion we will refer to these modes using abbreviations that are summarized in Table 1.

The event selection is developed from studies of simulated $B\overline{B}$ and continuum events, and off-resonance data. A large on-resonance control sample of $D\pi$ and $D^*\pi$ events is used to validate several aspects of the simulation and analysis procedure.

The analysis strategy is the following:

1. The goal is to measure or set limits on the charge-integrated ratios $\mathcal{R}_{K\pi}$ and $\mathcal{R}^*_{K\pi}$.

2. The first step consists in the application of a set of basic requirements to select possible candidate events, see Section 3.1.

3. After the basic requirements, the backgrounds are dominantly from continuum. These are significantly reduced using a neural network designed to distinguish between $B\overline{B}$ and continuum events, see Section 3.2.

4. After the neural network requirement, events are characterized by two kinematical variables that are customarily used when reconstructing B-meson decays at the $\Upsilon(4S)$. These variables are the energy-substituted mass, $m_{\rm ES} \equiv \sqrt{(\frac{s}{2} + \vec{p}_0 \cdot \vec{p}_B)^2/E_0^2 - p_B^2}$ and energy difference $\Delta E \equiv E_B^* - \frac{1}{2}\sqrt{s}$, where E and p are energy and momentum, the asterisk denotes the CM frame, the subscripts 0 and B refer to the $\Upsilon(4S)$ and B candidate, respectively, and s is the square of the CM energy. For signal events $m_{\rm ES} = m_B$ and $\Delta E = 0$ within the resolution of about 2.5 and 20 MeV respectively (here m_B is the known B mass).

5. We then perform simultaneous fits to the final signal samples ($\overline{D}K$ and $\overline{D}^*K$), the normalization samples (DK and D^*K), and the control samples ($D\pi$ and $D^*\pi$) to extract $\mathcal{R}_{K\pi}$ and $\mathcal{R}^*_{K\pi}$, see Section 3.3. The fits are based on the reconstructed values of $m_{\rm ES}$ and ΔE in the various event samples.

6. Throughout the whole analysis chain, care is taken to treat the signal, normalization, and control samples in a consistent manner.

3.1 Basic Requirements

Charged kaon and pion candidates in the decay modes of interest must satisfy K or π identification criteria [12] that are typically 85% efficient, depending on momentum and polar angle. The misidentification rates are at the few percent level. The invariant mass of the $K\pi$ pair must be within 18.8 MeV (2.5σ) of the mean reconstructed D^0 mass. For modes with $\overset{(-)}{D}{}^{*0} \to \overset{(-)}{D}{}^0\,\pi^0$ and $\overset{(-)}{D}{}^{*0} \to \overset{(-)}{D}{}^0\gamma$ the mass difference ΔM between the $\overset{(-)}{D}{}^{*0}$and the $\overset{(-)}{D}{}^0$must be within 3.5 (3.5σ) and 13 (2σ) MeV, respectively, of the expectation for $\overset{(-)}{D}{}^{*0}$decays.

A major background arises from DK and D^*K decays where the K and π in the D decay are misidentified as a π and a K respectively. When this happens, the decay could be reconstructed as $\overline{D}K$ or $\overline{D}^*K$ signal event. To eliminate this background, we recompute the invariant mass ($M_{\rm switch}$) of the h^+h^- pair in $\overset{(-)}{D}{}^0 \to h^+h^-$ switching the particle identification assumptions (π vs. K) on the h^+ and the h^-. We veto any candidates with $M_{\rm switch}$ consistent with the known D mass [13]. In the case of $\overset{(-)}{D}{}^0K$, we also veto any candidate where the $\overset{(-)}{D}{}^0$is consistent with D^* decay.

3.2 Neural Network

After these initial requirements, backgrounds are overwhelmingly from continuum events, especially $e^+e^- \to c\bar{c}$, with $\bar{c} \to \overline{D}^0X$, $\overline{D}^0 \to K^+\pi^-$ and $c \to DX$, $D \to K^-Y$.

The continuum background is reduced by using neural network techniques. The neural network algorithms used for the DK and $\overline{D}K$ modes are slightly different. First, we use for both modes a common neural network (NN) based on nine quantities that distinguish between continuum and $B\overline{B}$ events. Then, for the $\overline{D}^*K$ mode only, we also take advantage of the fact that the signal is distributed as $\cos^2\theta_{D^*}$ for $D^* \to D\pi$ or $\sin^2\theta_{D^*}$ for $D^* \to D\gamma$, while the background is roughly

independent of $\cos\theta_{D^*}$. Here θ_{D^*} is the decay angle of the D^*, *i.e.*, the angle between the direction of the D and the line of flight of the D^* relative to the parent B, evaluated in the D^* rest frame. Thus, we construct a second neural network, NN', which takes as inputs the output of NN and the value of $\cos\theta_{D^*}$. We then use as a selection requirement the output of NN in the $\overline{D}K$ analysis and the output of NN' in the $\overline{D}^*K$ analysis.

The nine variables used in defining NN are the following:

1. A Fisher discriminant constructed from the quantities $L_0 = \sum_i p_i$ and $L_2 = \sum_i p_i \cos^2\theta_i$ calculated in the CM frame. Here, p_i is the momentum and θ_i is the angle with respect to the thrust axis of the B candidate of tracks and clusters not used to reconstruct the B meson.

2. $|\cos\theta_T|$, where θ_T is the angle in the CM frame between the thrust axes of the B candidate and the detected remainder of the event. The distribution of $|\cos\theta_T|$ is approximately flat for signal and strongly peaked at one for continuum background.

3. $\cos\theta_B$, where θ_B is the polar angle of the B candidate in the CM frame. In this variable, the signal follows a $\sin^2\theta_B$ distribution, while the background is approximately uniform.

4. $\cos\theta_D^K$ where θ_D^K is the decay angle in $\overline{(}D^{0)} \to K\pi$.

5. $\cos\theta_B^D$, where θ_B^D is the decay angle in $B \to \overline{(}D^{0)}K$ or $B \to \overline{(}D^{*0)}K$.

6. The charge difference ΔQ between the sum of the charges of tracks in the $\overline{(}D^{0)}$ or $\overline{(}D^{*0)}$ hemisphere and the sum of the charges of the tracks in the opposite hemisphere excluding the tracks used in the reconstructed B. For signal, $\langle\Delta Q\rangle = 0$, whereas for the $c\bar{c}$ background $\langle\Delta Q\rangle \approx \frac{7}{3} \times Q_B$, where Q_B is the charge of the B candidate. The ΔQ RMS is 2.4.

7. $Q_B \cdot Q_K$, where Q_K is the sum of the charges of all kaons not in the reconstructed B. In many signal events, there is a charged kaon among the decay products of the other B in the event. The charge of this kaon tends to be highly correlated with the charge of the B. Thus, signal events tend to have $Q_B \cdot Q_K \leq -1$. On the other hand, most continuum events have no kaons outside of the reconstructed B, and therefore $Q_K = 0$.

8. The distance of closest approach between the bachelor track and the trajectory of the $\overline{(}D^{0)}$. This is consistent with zero for signal events, but can be larger in $c\bar{c}$ events.

9. The existence of a lepton (e or μ) and the invariant mass ($m_{K\ell}$) of this lepton and the bachelor K. Continuum events have fewer leptons than signal events. Furthermore, a large fraction of leptons in $c\bar{c}$ events are from $D \to K\ell\nu$, where K is the bachelor kaon, so that $m_{K\ell} < m_D$.

The neural networks (NN and NN') are trained with simulated continuum and signal events. The distributions of the NN and NN' outputs for the control samples ($D\pi$, $D^*\pi$, and off resonance data), are compared with expectations from the Monte Carlo simulation in Figure 2. The agreement is satisfactory. We have also examined the distributions of all variables used in NN and NN', and found good agreement between the simulation and the data control samples.

Our final events selection requirement is $NN > 0.5$ for $\overline{D}K$ and $NN' > 0.5$ for $\overline{D}^*K$. In addition, to reduce the remaining $B\overline{B}$ backgrounds, we also require $\cos\theta_D^K > -0.75$. These requirements are about 40% efficient on simulated signal events, and reject 98.5% of the continuum background. Note, however, that we do not rely on the Monte Carlo simulation to estimate the efficiency of the

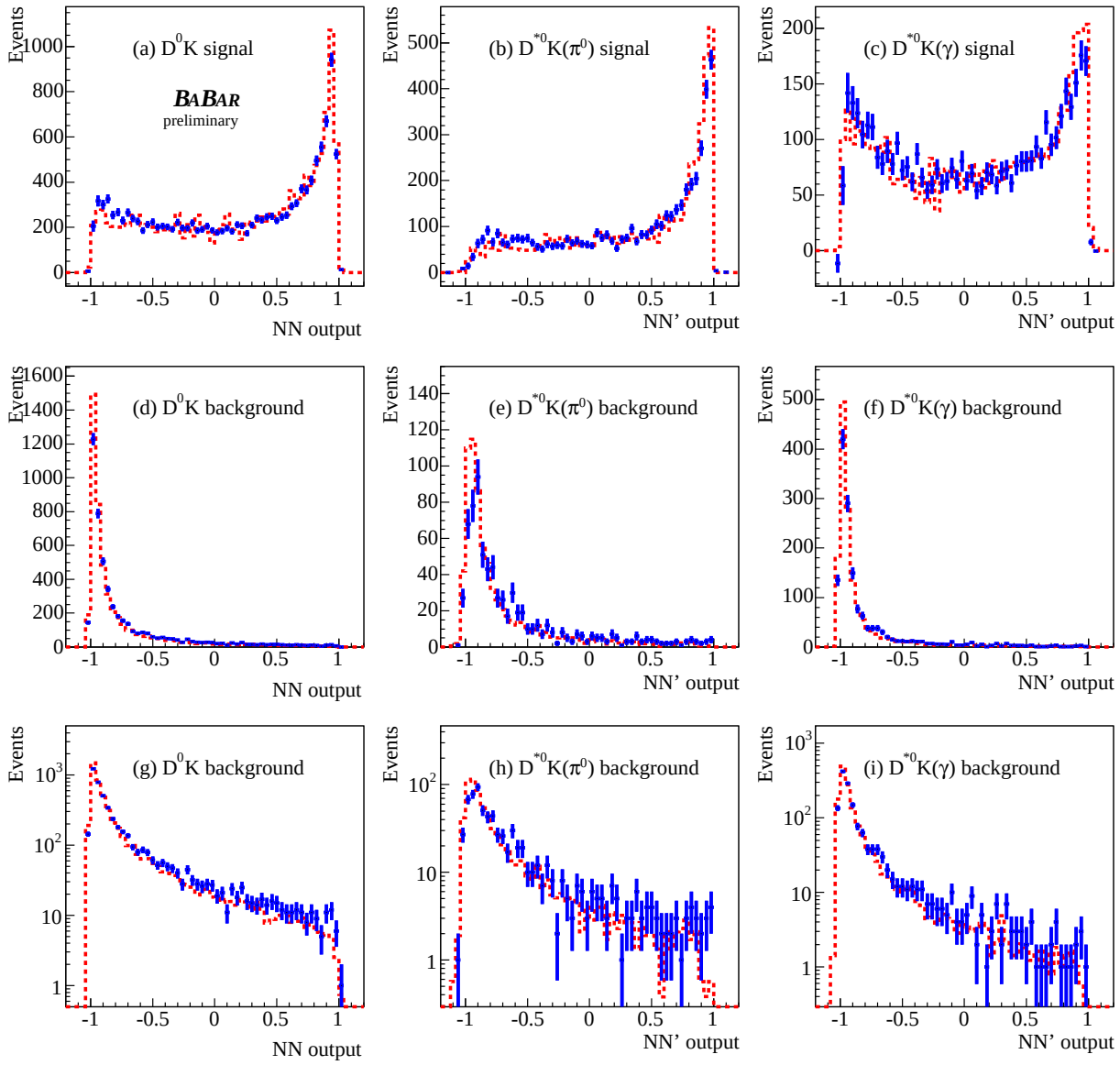

Figure 2: Distributions of the continuum suppression neural network (NN and NN') outputs for the three modes. Figures (a-c) show the expected distribution from signal events. The solid line histogram shows the distribution of simulated signal events, the histogram with error bars shows the distribution of $D^{(*)0}\pi$ control sample events with background subtracted using the $m_{\rm ES}$ sideband. Figures (d-i) show the expected distribution for continuum background events. The solid line histogram shows the distribution of simulated continuum events and the histogram with errors show the distribution of off-resonance events. The $m_{\rm ES}$ and ΔE requirements on the off-resonance and continuum Monte Carlo events have been kept loose to increase the statistics. Figures (g-i) show the distributions of figures (d-g) in log scale. Each Monte Carlo histogram is normalized to the area of the corresponding data histogram.

neural net requirements. We apply the exact same requirements to the normalization modes DK and D^*K. Then, in the extraction of $\mathcal{R}_{K\pi}$ and $\mathcal{R}^*_{K\pi}$, the efficiencies of the overall selection cancels in the ratio.

3.3 Fitting for event yields and $\mathcal{R}^{(*)}_{\mathcal{K}\pi}$

The ratios $\mathcal{R}_{\mathcal{K}\pi}$ and $\mathcal{R}^*_{\mathcal{K}\pi}$ are extracted from the ratios of the event yields in the m_{ES} distribution for the signal modes ($\overline{D}K$ and $\overline{D}^*K$) and the normalization modes (DK and D^*K), while taking into account potential differences in efficiencies and backgrounds. All events must satisfy the requirements discussed above and have a ΔE value consistent with zero within the resolution (-52 MeV $< \Delta E <$ 44 MeV).

The $m_{\rm ES}$ distributions for $\overline{D}K$ (signal mode) and DK (normalization mode) are fitted simultaneously. The fit parameter $\mathcal{R}_{K\pi}$ is given by $\mathcal{R}_{K\pi} \equiv c \cdot N_{\overline{D}K}/N_{DK}$, where $N_{\overline{D}K}$ and N_{DK} are the fitted yields of $\overline{D}K$ and DK events, and c is a correction factor, determined from Monte Carlo, for the ratio of efficiencies between the two modes. We find that this factor c is consistent with unity within the statistical accuracy of the simulation, $c = 0.98 \pm 0.04$[6].

The $m_{\rm ES}$ distributions are modeled as the sum of a threshold combinatorial background function [14] and a Gaussian centered at m_B. The parameters of the background function for the signal mode are constrained by a simultaneous fit of the $m_{\rm ES}$ distribution for events in the sideband of ΔE (-120 MeV $< \Delta E <$ 200 MeV, excluding the ΔE signal region defined above). The parameters of the Gaussian for the signal and normalization modes are constrained to be identical. The number of events in the Gaussian is $N_{sig} + N_{peak}$, where $N_{sig} = N_{DK}$ or $N_{\overline{D}K}$ and N_{peak} is the number of background events expected to be distributed in the same way as the DK or $\overline{D}K$ in $m_{\rm ES}$ ("peaking backgrounds").

There are two classes of peaking background events:

1. Charmless B decays, *e.g.*, $B^- \to K^+K^-\pi^+$. These are indistinguishable from the $\overline{D}K$ signal if the $K^-\pi^+$ pair happens to be consistent with the D-mass.

2. Events of the type $B^- \to D^0\pi^-$ ($D\pi$), where the bachelor π^- is misidentified as a K^-. When the D^0 decays into $K^-\pi^+$ ($K^+\pi^-$), these events are indistinguishable in $m_{\rm ES}$ from DK ($\overline{D}K$), since $m_{\rm ES}$ is insensitive to particle identification assumptions.

The amount of charmless background (1) is estimated directly from the data by performing a simultaneous fit to events in the sideband of the reconstructed D mass. The ΔE distribution of the $D\pi$ background (2) is shifted by about +50 MeV due to the misidentification of the bachelor π as a K. Since the ΔE resolution is of order 20 MeV, the ΔE requirement does not eliminate this background completely. The remaining $D\pi$ background after the ΔE requirement is estimated from a fit to the ΔE distribution of the DK sample.

We fit the ΔE distribution of DK candidates, with $m_{\rm ES}$ within 3σ of m_B, to the sum of a DK component, a $D\pi$ component, and a combinatorial component. The $D\pi$ sample, with the bachelor track identified as a pion, is used to constrain the shape of the DK component in the DK sample. The same sample of $D\pi$ events, but reconstructed as DK events, is used to constrain the shape of the $D\pi$ background in the DK sample. The fitted number of $D\pi$ background events in this

[6] In the D^* modes this correction factor is $c = 0.97 \pm 0.05$ and $c = 0.99 \pm 0.05$ for $D^* \to D\pi^0$ and $D^* \to D\gamma$ respectively.

sample that survive the ΔE requirements, which we denote as N^{π}_{DK}, is taken as the number of $D\pi$ background events in the fit to the m_{ES} distribution of DK events..

The $D\pi$ peaking background is much more important in the DK (normalization) channel than in the $\overline{D}K$ (signal) channel. This is because in order to contribute to the signal channel, the D^0 has to decay into $K^+\pi^-$, and this mode is doubly Cabibbo-suppressed. For the $\overline{D}K$ (signal) sample, the contribution from the residual $D\pi$ peaking background in the $m_{\rm ES}$ fit is estimated as $N^{\pi}_{\overline{D}K} = r_D^2 N^{\pi}_{DK}$, where $r_D = 0.060 \pm 0.003$ is the ratio of the doubly Cabibbo-suppressed to the Cabibbo-favored $D \to K\pi$ amplitudes (see Eq. 5), and N^{π}_{DK} was defined above.

The complete procedure simultaneously fits seven distributions: the m_{ES} distributions of DK and $\overline{D}K$, the $\overline{D}K$ distributions in sidebands of ΔE and $m(D^0)$, the ΔE distribution of DK, and the ΔE distributions of $D\pi$ reconstructed as $D\pi$ and as DK. The fits are configured in such a way that $\mathcal{R}_{\mathcal{K}\pi}$ and $\mathcal{R}^*_{\mathcal{K}\pi}$ are explicit fit parameters. The advantage of this approach is that all uncertainties, including the uncertainties in the PDFs and the uncertainties in the background subtractions, are automatically correctly propagated in the statistical uncertainty reported by the fit.

The fit is performed separately for $\overline{D}K$, $\overline{D}^*K$, $\overline{D}^* \to \overline{D}\pi^0$, and $\overline{D}^*K$, $\overline{D}^* \to \overline{D}\gamma$ and is identical for all three modes, except in the choice of parameterization for some signal and background components in the ΔE fits.

Systematic uncertainties in the detector efficiency cancel in the ratio. This cancellation has been verified by studies of simulated events, with a statistical precision of a few per-cent. The likelihood includes a Gaussian uncertainty term for this cancellation which is set by the statistical accuracy of the simulation. Other systematic uncertainties, e.g., the uncertainty in the parameter r_D which is used to estimate the amount of peaking backgrounds from $D^{(*)}\pi$, are also included in the formulation of the likelihood.

The fit procedure has been extensively tested on sets of simulated events. It was found to provide an unbiased estimation of the parameters $\mathcal{R}_{\mathcal{K}\pi}$ and $\mathcal{R}^*_{\mathcal{K}\pi}$.

4 RESULTS

The results of the fits are displayed in Table 2 and Figs. 3, 4, 5, and 6. As is apparent from Fig. 6, we see no evidence for the $\overline{D}^*K$ modes and no significant evidence for the $\overline{D}K$ mode.

For the $\overline{D}K$ mode we find $\mathcal{R}_{\mathcal{K}\pi} = 13^{+11}_{-9} \times 10^{-3}$; For the $\overline{D}^*K$ mode we find $\mathcal{R}^*_{\mathcal{K}\pi} = -1^{+10}_{-6} \times 10^{-3}$ (for $D^* \to D\pi^0$) and $\mathcal{R}^*_{\mathcal{K}\pi} = 11^{+19}_{-13} \times 10^{-3}$ (for $D^* \to D\gamma$). Results for the two $\overline{D}^*K$ submodes are combined by multiplying the two likelihoods, ignoring the very small correlation between the two $\mathcal{R}^*_{\mathcal{K}\pi}$ measurements from the uncertainty on r_D. The combined result is then $\mathcal{R}^*_{\mathcal{K}\pi} = 3^{+10}_{-7} \times 10^{-3}$. We estimate from a parameterized Monte Carlo study that the probability that an upward fluctuation of background events results in our observed value of $\mathcal{R}_{\mathcal{K}\pi}$ or larger is 7.5%.

From the likelihoods as a function of $\mathcal{R}_{\mathcal{K}\pi}$ and $\mathcal{R}^*_{\mathcal{K}\pi}$ (see Figure 7), we set upper limits on $\mathcal{R}_{\mathcal{K}\pi}$ and $\mathcal{R}^*_{\mathcal{K}\pi}$ using a Bayesian method with a uniform prior for $\mathcal{R}^{(*)}_{\mathcal{K}\pi} > 0$. These limits are $\mathcal{R}_{\mathcal{K}\pi} < 0.030$ and $\mathcal{R}^*_{\mathcal{K}\pi} < 0.021$ at 90% C.L..

In Fig. 8 we show the dependence of $\mathcal{R}^{(*)}_{K\pi}$ on $r_B^{(*)}$, together with our limits. These are shown allowing a $\pm 1\sigma$ variation on r_D, for the full range $0^\circ - 180^\circ$ for γ and $\delta^{(*)}$, as well as with the restriction $48^\circ < \gamma < 73^\circ$ suggested by global CKM fits [15]. The least restrictive limits on r_B and r_B^* are computed assuming maximal destructive interference: $\gamma = 0^\circ, \delta^{(*)} = 180^\circ$ or $\gamma = 180^\circ, \delta^{(*)} = 0^\circ$. These limits are $r_B < 0.23$ and $r_B^* < 0.21$ at 90% C.L..

Table 2: Summary of fit results.

Mode	$\overline{D}K$	$\overline{D}^*K$, $\overline{D}^* \to \overline{D}\pi^0$	$\overline{D}^*K$, $\overline{D}^* \to \overline{D}\gamma$
Ratio of rates, $\mathcal{R}_{\mathcal{K}\pi}$ or $\mathcal{R}^*_{\mathcal{K}\pi}$, $\times 10^{-3}$	$\mathcal{R}_{\mathcal{K}\pi} = 13^{+11}_{-9}$	$\mathcal{R}^*_{\mathcal{K}\pi} = -1^{+10}_{-6}$	$\mathcal{R}^*_{\mathcal{K}\pi} = 11^{+19}_{-13}$
No. of signal events	$4.7^{+4.0}_{-3.2}$	$-0.2^{+1.3}_{-0.8}$	$1.2^{+2.1}_{-1.4}$
No. of normalization events	356 ± 26	142 ± 17	101 ± 14
No. of peaking charmless events	$0.75^{+1.3}_{-0.75}$	$0^{+0.3}_{-0.0}$	$0.05^{+0.7}_{0.05}$
No. of peaking $D^{(*)}\pi$ ev. in sig. sample	0.47 ± 0.04	0.17 ± 0.02	$0.01^{+0.03}_{-0}$
No. of peaking $D^{(*)}\pi$ ev. in norm. sample	132 ± 10	48 ± 6	2.5 ± 8

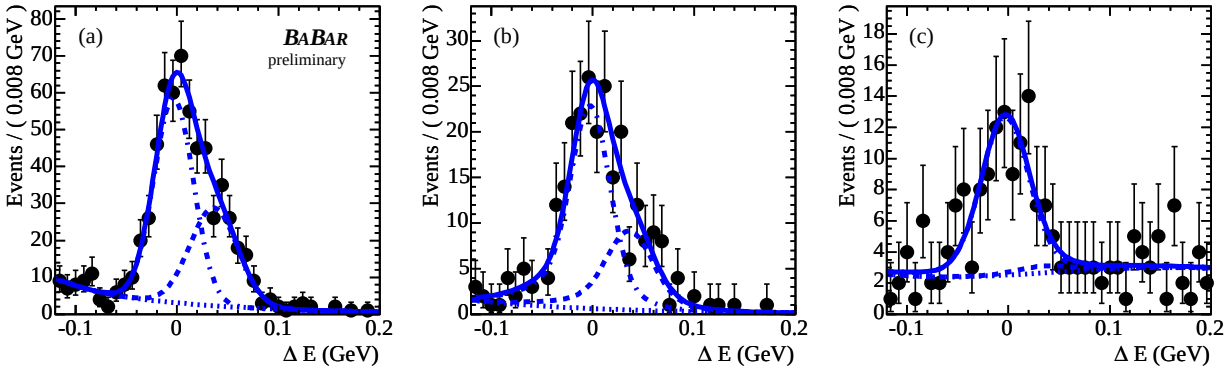

Figure 3: ΔE distributions for normalization events (DK and D^*K) with $m_{\rm ES}$ within 3σ of m_B with the fit model overlaid. (a) DK events. (b) D^*K events with $D^* \to D\pi^0$. (c) D^*K events with $D^* \to D\gamma$. The dashed (dot-dashed) curves are the contributions from $D\pi$ or $D^*\pi$ (DK or D^*K) events. The dotted curves are the contributions from other backgrounds, and the solid line is the total.

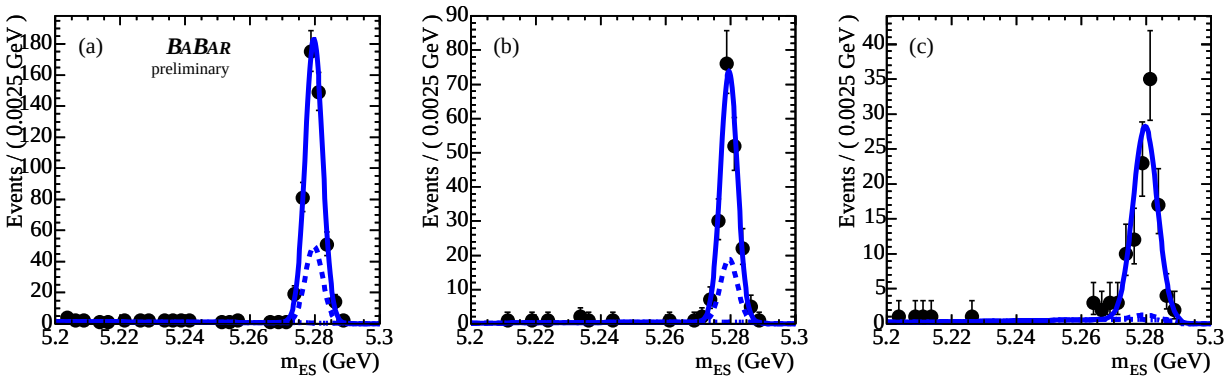

Figure 4: $m_{\rm ES}$ distributions for normalization events (DK and D^*K) with ΔE in the signal region with the fit model overlaid. (a) DK events. (b) D^*K events with $D^* \to D\pi^0$. (c) D^*K events with $D^* \to D\gamma$. The dashed curves represent the backgrounds; these are mostly from $D\pi$ or $D^*\pi$, and also peak at the B-mass. As explained in the text, the size of the $D\pi$ and $D^*\pi$ backgrounds is constrained by the simultaneous fits to the distributions of Figure 3.

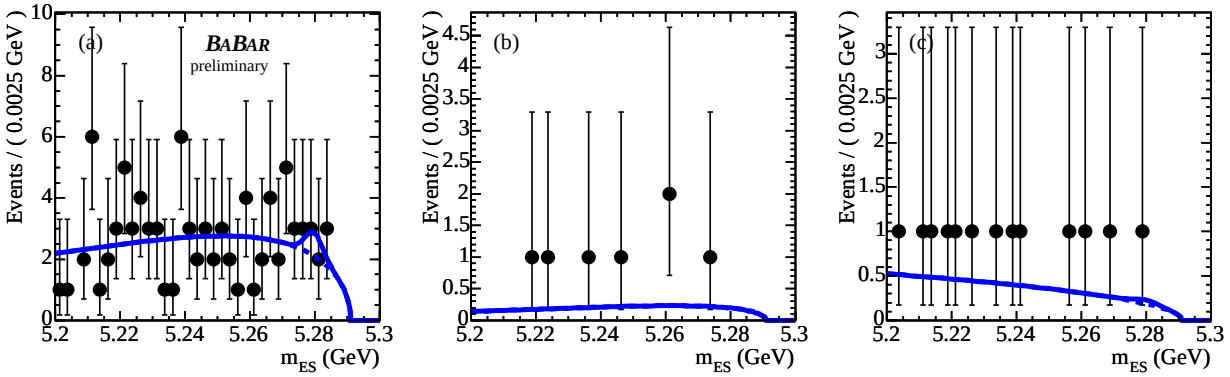

Figure 5: $m_{\rm ES}$ distributions for $\overline{D}K$ and $\overline{D}^*K$ events with $K\pi$ mass in a sideband of the reconstructed D mass and with ΔE in the signal region. These events are used to constrain the size of possible peaking backgrounds from charmless B-meson decays, *i.e.*, decays without a D in the final state. The fit model is overlaid. (a) $\overline{D}K$ events. (b) $\overline{D}^*K$ events with $D^* \to D\pi^0$. (c) $\overline{D}^*K$ events with $D^* \to D\gamma$. Note that the $K\pi$ mass range in the sideband selection is a factor of 2.7 larger than in the signal selection.

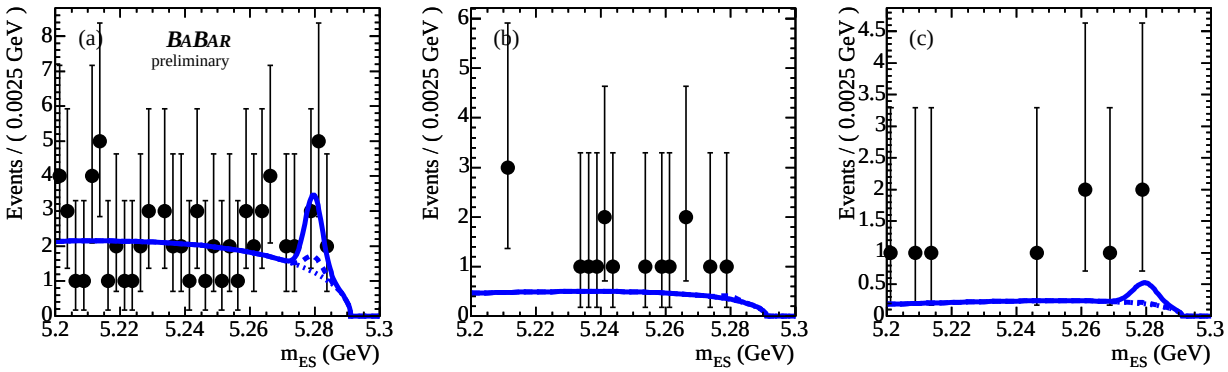

Figure 6: $m_{\rm ES}$ distributions for candidate signal events with the fit model overlaid. (a) $\overline{D}K$ events. (b) $\overline{D}^*K$ events with $D^* \to D\pi^0$. (c) $\overline{D}^*K$ events with $D^* \to D\gamma$.

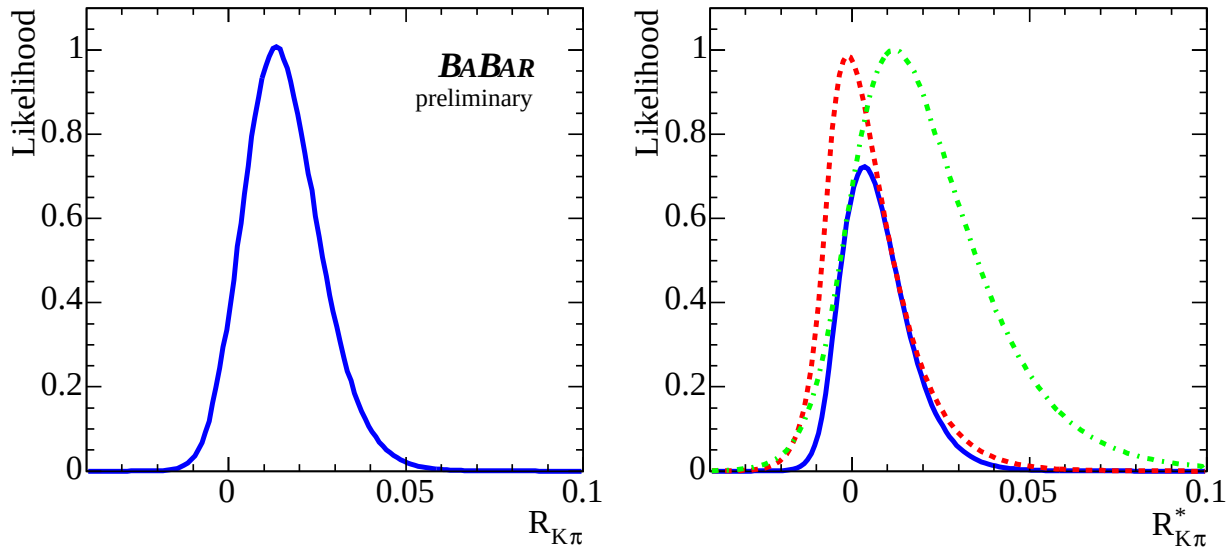

Figure 7: Likelihood distributions (arbitrary units) for $\mathcal{R}_{\mathcal{K}\pi}$ (left plot) and $\mathcal{R}^*_{\mathcal{K}\pi}$ (right plot). For $\mathcal{R}^*_{\mathcal{K}\pi}$ we show three curves: red dashed for $D^* \to D\pi^0$, green dot-dashed for $D^* \to D\gamma$, solid blue for the combination of the two.

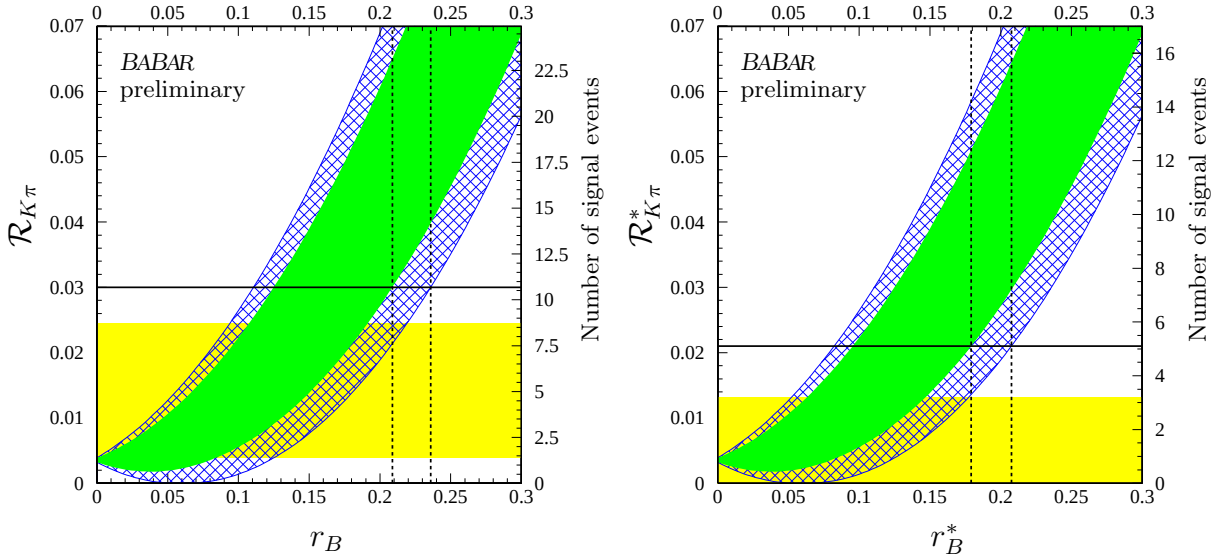

Figure 8: Expectations for $\mathcal{R}^{(*)}_{K\pi}$ and the number of signal events *vs.* $r^{(*)}_B$). Dark filled-in areas: allowed regions for any value of $\delta^{(*)}$, with a $\pm 1\sigma$ variation on r_D, and $48^\circ < \gamma < 73^\circ$. Hatched area: additional allowed regions with no constraint on γ. Note that the uncertainty on r_D has a very small effect on the size of the allowed regions. The horizontal lines represents the 90% C.L. limit $\mathcal{R}_{K\pi} < 0.030$ and $\mathcal{R}^*_{K\pi} < 0.021$ The vertical dashed lines are drawn at $r_B = 0.209$, $r_B = 0.235$, $r^*_B = 0.179$, and $r^*_B = 0.208$. They represent the 90% C.L. upper limits on r_B and r^*_B with and without the constraint on γ. The light filled in areas represent the 68% C.L. regions corresponding to $\mathcal{R}_{K\pi} = 0.013 \pm^{0.011}_{0.009}$ and $\mathcal{R}^*_{K\pi} = 0.003 \pm^{0.010}_{0.007}$.

5 SUMMARY

In summary, we find no significant evidence for the decay $B^\pm \to [K^\mp\pi^\pm]_D K^\pm$ and no evidence for the decay $B^\pm \to [K^\mp\pi^\pm]_{D^*} K^\pm$. We set 90% C.L. limits on the ratios $\mathcal{R}_{K\pi}$ and $\mathcal{R}^*_{K\pi}$ of rates for this mode and the favored modes $B^\pm \to [K^\pm\pi^\mp]_D K^\pm$ and $B^\pm \to [K^\pm\pi^\mp]_{D^*} K^\pm$. Our preliminary results are

$$\mathcal{R}_{K\pi} < 0.030 \quad (90\% \text{ C.L.})$$

$$\mathcal{R}^*_{K\pi} < 0.021 \quad (90\% \text{ C.L.}),$$

where the central values are $\mathcal{R}_{K\pi} = 0.013 \pm^{0.011}_{0.009}$ and $\mathcal{R}^*_{K\pi} = 0.003 \pm^{0.010}_{0.007}$. With the most conservative assumption on the values of γ and of the strong phases in the B and D decays, these translate into limits on the ratio of the magnitudes of the $B^- \to \overline{D}^{(*)0} K^-$ and $B^- \to D^{(*)0} K^-$ amplitudes $r_B < 0.23$ and $r^*_B < 0.21$ at 90% C.L.. If r_B and r^*_B are small, as our analysis suggests, the suppression of the $b \to u$ amplitude will make the determination of γ using methods based on the interference of the diagrams in Figure 1 difficult.

6 ACKNOWLEDGMENTS

We are grateful for the extraordinary contributions of our PEP-II colleagues in achieving the excellent luminosity and machine conditions that have made this work possible. The success of this project also relies critically on the expertise and dedication of the computing organizations that support *BABAR*. The collaborating institutions wish to thank SLAC for its support and the kind hospitality extended to them. This work is supported by the US Department of Energy and National Science Foundation, the Natural Sciences and Engineering Research Council (Canada), Institute of High Energy Physics (China), the Commissariat à l'Energie Atomique and Institut National de Physique Nucléaire et de Physique des Particules (France), the Bundesministerium für Bildung und Forschung and Deutsche Forschungsgemeinschaft (Germany), the Istituto Nazionale di Fisica Nucleare (Italy), the Foundation for Fundamental Research on Matter (The Netherlands), the Research Council of Norway, the Ministry of Science and Technology of the Russian Federation, and the Particle Physics and Astronomy Research Council (United Kingdom). Individuals have received support from CONACyT (Mexico), the A. P. Sloan Foundation, the Research Corporation, and the Alexander von Humboldt Foundation.

References

[1] *BABAR* Collaboration, B. Aubert *et al.*, Phys. Rev. Lett. **89**, 201802 (2002); Belle Collaboration, K. Abe *et al.*, Phys. Rev. **D66**, 071102 (2002).

[2] L. Wolfenstein, Phys. Rev. Lett. **51**, 1945 (1983).

[3] M. Gronau and D. Wyler, Phys. Lett. **B265**, 172 (1991); M. Gronau and D. London, Phys. Lett. **B253**, 483 (1991).

[4] D. Atwood, I. Dunietz, and A. Soni, Phys. Rev. Lett. **78**, 3257 (1997); Phys. Rev. **D63**, 036005 (2001).

[5] *BABAR* Collaboration, B. Aubert *et al.*, Phys. Rev. Lett. **91**, 171801 (2003).

[6] See, for example, M. Neubert and B. Stech, in *Heavy Flavors, 2nd Edition*, edited by A.J. Buras and M. Lindner, World Scientific, Singapore, 1997.

[7] CLEO Collaboration, T.E. Coan *et al.*, Phys. Rev. Lett. **88**, 062001 (2001). Belle Collaboration, K. Abe *et al.*, Phys. Rev. Lett. **88**, 052002 (2002); A. Satpathy *et al.*, Phys. Lett. **B553**, 159 (2003). *BABAR* Collaboration, B. Aubert *et al.*, Phys. Rev. **D69**, 032004 (2004).

[8] *BABAR* Collaboration, B. Aubert *et al.*, `hep-ex/0402024`.

[9] Belle Collaboration, K. Abe *et al.*, `hep-ex/0406067`.

[10] *BABAR* Collaboration, B. Aubert *et al.*, Nucl. Instr. and Methods **A479**, 1 (2002).

[11] PEP-II Conceptual Design Report, SLAC-0418 (1993).

[12] *BABAR* Collaboration, B. Aubert *et al.*, Phys. Rev. **D66**, 032003 (2002).

[13] Particle Data Group, S. Eidelman et al., Phys. Lett. B592, 1 (2004).

[14] The function is $f(m_{ES}) \propto m_{ES}\sqrt{1-x^2}\exp[-\zeta(1-x^2)]$, where $x = 2m_{ES}/\sqrt{s}$; ARGUS Collaboration, H. Albrecht *et al.*, Z. Phys. **C48**, 543 (1990).

[15] A. Höcker, H. Lacker, S. Laplace, and F. Le Diberder, Eur. Phys. J. **C21**, 225 (2001); updated results can be found in `http://ckmfitter.in2p3.fr`.